

2009

Period fissioning and other instabilities of stressed elastic membranes

B Davidovitch

University of Massachusetts - Amherst, bdavidov@physics.umass.edu

Follow this and additional works at: http://scholarworks.umass.edu/physics_faculty_pubs



Part of the [Physics Commons](#)

Recommended Citation

Davidovitch, B, "Period fissioning and other instabilities of stressed elastic membranes" (2009). *Physics Review E*. 1100.
http://scholarworks.umass.edu/physics_faculty_pubs/1100

This Article is brought to you for free and open access by the Physics at ScholarWorks@UMass Amherst. It has been accepted for inclusion in Physics Department Faculty Publication Series by an authorized administrator of ScholarWorks@UMass Amherst. For more information, please contact scholarworks@library.umass.edu.

Period fissioning and other instabilities of stressed elastic membranes

Benny Davidovitch

Physics Department, University of Massachusetts, Amherst MA 01003

(Dated: January 18, 2009)

We study the shapes of elastic membranes under the simultaneous exertion of tensile and compressive forces when the translational symmetry along the tension direction is broken. We predict a multitude of novel morphological phases in various regimes of a 2-dimensional parameter space (ϵ, ν) that defines the relevant mechanical and geometrical conditions. These parameters are, respectively, the ratio between compression and tension, and the wavelength contrast along the tension direction. In particular, our theory associates the repetitive increase of pattern periodicity, recently observed on wrinkled membranes floating on liquid and subject to capillary forces, to the morphology in the regime $(\epsilon \ll 1, \nu \gg 1)$ where tension is dominant and the wavelength contrast is large.

Thin membranes, such as paper sheets, tend to buckle when compressive forces are exerted on their boundaries. The origin of this familiar phenomenon, known as Euler instability, is the large contrast between the energetic costs of straining and strain-free bending of thin elastic bodies. This feature is reflected in the different dependencies of the bending modulus $B \sim Et^3$ and stretching modulus $Y \sim Et$ on the Young modulus E and thickness t of the membrane [1]. Wrinkling patterns, which often appear on supported membranes such as human skin or milk crusts, are characterized by a buckling scale l_0 that can be much smaller than the membrane width W in the compression direction. Here, the distortion of the attached substrate gives rise to an energetic cost that is proportional to the amplitude ζ_0 of the bent shape, and the formation of a 1-dimensional (1d) periodic wrinkling pattern is induced by balancing restoring forces associated with this distortion and with bending resistivity of the membrane [2]. Near buckling (wrinkling) threshold, the ratio $\tilde{\Delta} = \Delta/W$ between the displacement Δ and width W is small (see Fig. 1), and the membrane attains a sinusoidal shape whose wavelength and amplitude are:

$$(a) l_0 = \sqrt{\frac{B}{|\sigma_{yy}|}} \quad ; \quad (b) \frac{\zeta_0}{l_0} = \sqrt{\tilde{\Delta}}/\pi \quad (1)$$

where $\sigma_{yy} < 0$ is the compressive stress, and the *inextensibility* criterion (1b) reflects the conservation of the contour length of material lines along the compression direction \hat{y} . This description corresponds to situations in which the exerted forces are purely compressive and enable the formation of a 1d shape. This ideal picture

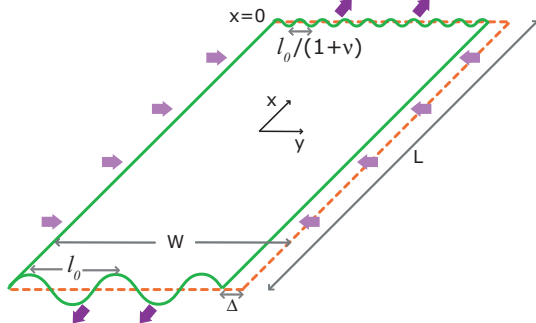


FIG. 1: Membrane geometry studied in this Letter.

can be qualitatively modified when: (1) the translational symmetry along the orthogonal direction (\hat{x}) is broken, or: (2) when tension $\sigma_{xx} = T$ is exerted on the membrane. The dramatic effect of symmetry breaking can be demonstrated by considering a bent membrane, whose amplitude $\zeta(x, y)$ is forced to assume a sinusoidal shape of wavelength $l_e = l_0/(1 + \nu)$ at the uncompressed edge ($x=0$), where ν is the *wavelength contrast*. As the inextensibility criterion (1b) shows, the limit $\nu \rightarrow \infty$ corresponds to a vanishing amplitude $\zeta_e \rightarrow 0$ at the edge, a geometry similar to the "curtain problem" studied by Pomeau and Rica [3]. As was shown in [3], the transition from the vanishing amplitude at $x=0$ to the finite value ζ_0 , Eq. (1b), is characterized by a cascade of sharp folds whose lengths may become infinitesimally small as $x \rightarrow 0$. The important role of tension was recently noticed by Cerda and Mahadevan [2], who showed that exerting tension $\sigma_{xx} = T$ on a membrane with length L and free edges at $y=0, W$ implies a small compression $|\sigma_{yy}| \sim (t/L)T$ that may induce a periodic wrinkling pattern in the \hat{y} direction. A useful number for characterizing tensile effects on wrinkling phenomena is the *stress ratio* $\epsilon = |\sigma_{yy}|/\sigma_{xx}$.

In this Letter we classify the morphologies of elastic membranes for general values of the pair of parameters (ϵ, ν) near buckling (wrinkling) threshold ($\tilde{\Delta} \ll 1$). Our theory reveals a surprisingly rich phase space, and in particular predicts the existence of novel types of *smooth cascades*, qualitatively different from the hierarchy of sharp folds found in [3]. Our interest in this problem was triggered by the repetitive increase of wrinkles periodicity in discrete steps, that was recently observed near the uncompressed edges ($x=-L, 0$) of ultrathin membranes floating on liquid surface and compressed along \hat{y} with $\tilde{\Delta} \ll 1$ [4]. As was realized in [4], these membranes are under large tension σ_{xx} , and the amplitude ζ_e at their uncompressed edges is suppressed due to the high energetic cost of the liquid-vapor menisci (at $x > 0, x < -L$), induced by the bent membrane. The experimental conditions in [4] thus correspond to the asymptotic regime $(\epsilon \ll 1, \nu \gg 1)$, which is the main focus of this Letter.

Our geometry is depicted in Fig. 1. It is similar to the one studied in [3] with three crucial differences: (i) The displacement Δ in the \hat{y} direction is assumed constant (rather than constant compression $\sigma_{yy} = P$). (ii) The

tension $\sigma_{xx}=T$ in \hat{x} is assumed constant (rather than constant length L), and **(iii)** The wavelength contrast ν can be any positive number (rather than $\nu \rightarrow \infty$). In order to describe the wrinkling patterns of [4], we assume the membrane is floating on liquid, and include the energetic cost of the lifted liquid mass of density ρ induced by the bent membrane. Our formalism and results are generalizable, however, to wrinkling problems in which gravity is replaced by another restoring force (e.g. due to an attached elastic substrate) or if bending is the only energetic cost (i.e. buckling). To quadratic order in $\tilde{\Delta}$, the areal energy density of a shape $\zeta(x, y)$ is [4]:

$$u = \frac{1}{2} \left(B(\nabla^2 \zeta)^2 + \rho g \zeta^2 + \sigma(x) \left[\left(\frac{\partial \zeta}{\partial y} \right)^2 - 2\tilde{\Delta} \right] + T \left(\frac{\partial \zeta}{\partial x} \right)^2 \right) \quad (2)$$

where $\sigma(x)$, the compressive stress σ_{yy} that must be exerted at $y=0, W$ in order to impose a constant $\tilde{\Delta}$, appears as a Lagrange multiplier that forces *inextensibility* of contour lines parallel to the \hat{y} direction. Let us briefly review the case of a free uncompressed edge $y = 0$ [4, 5]. The energy is then minimized by the 1d periodic pattern:

$$(a) \zeta(x, y) = \zeta \sin(qy) \quad ; \quad (b) \zeta = \frac{2}{q} \sqrt{\tilde{\Delta}} \quad (3)$$

with $q = q_0 \equiv (\rho g/B)^{1/4}$ and $\sigma_{yy} = \sigma_0 = -2\sqrt{B\rho g}$. The parameter ϵ is hence defined as the ratio $\epsilon \equiv \sigma_0/T$. The energy of the shape (3) is the work $\sigma_0 \Delta L$, whereas the *in-plane* compression energy is $\frac{1}{2} Y \tilde{\Delta}^2 W L$. One thus obtains the threshold value $\tilde{\Delta}_{min} = 2\sigma_0/Y$, below which the membrane does not bend. Consider now the case in which the edge $x=0$ is forced to take an unstrained periodic shape (3b) with a wavenumber $q_e = (1+\nu)q_0$. We assume the length L is sufficiently large such that away from the forced edge at $x=0$ the membrane fully recovers its energetically favorable form (3a) with $q=q_0$. A natural guess for the shape is then the superposition:

$$\zeta(x, y) = \zeta_0(x) \sin(q_0 y) + \zeta_1(x) \sin(q_1 y) \quad , \quad (4)$$

$$\text{where: } q_0^2 \zeta_0^2 + q_1^2 \zeta_1^2 = 4\tilde{\Delta} \quad , \quad (5)$$

$$\text{and: (a) } \lim_{x \rightarrow X_0} \zeta_1(x) = 0 \quad ; \quad (b) \lim_{x \rightarrow X_1} \zeta_0(x) = 0 \quad , \quad (6)$$

where (5) is the inextensibility condition (recall that $\tilde{\Delta} \ll 1$), and $X_0, X_1 = -L, 0$, respectively, and similarly $q_1 = q_e$ are introduced to simplify the forthcoming analysis. Notice that the superposition (4) constitutes the *most symmetric* shape possible under the boundary conditions (BC), Eq. (6). Obviously, such a smooth shape is markedly different from the irregular one described in [3] in the tensionless case ($T=0$). This difference stems from the Gaussian curvature imposed in the membrane by a wavelength contrast $\nu > 0$, and the associated *anharmonic* energy density u_G whose minimization (for $T=0$) gives rise to stress focusing at ridges and vertices which relieves the strain at all other areas of the distorted membrane [6]. This principle underlies the emergence of sharp folds in the tensionless limit $\epsilon \rightarrow 0$ [3]. Assuming for the smooth

shape (4) $\partial_x \zeta_i \sim \zeta_i/l$, with some typical length l , one obtains $u_G \sim Y l^{-2} \sum_i \zeta_i^4 q_i^2$ [6, 7]. For $T = \delta \cdot Y \neq 0$ the situation is different since even regions free from Gaussian curvature are penalized by the term $u_T = T(\partial_x \zeta)^2 \sim T l^{-2} \sum_i \zeta_i^2$. A transition from an irregular shape (at $\epsilon \rightarrow 0$) to a smooth one (4) is thus expected if $u_T > u_G$. With Eq. (5) this inequality implies: $\tilde{\Delta} \lesssim \delta$. Recalling the threshold condition $\tilde{\Delta} \gtrsim \sigma_0/Y$, we obtain a necessary condition for the existence of a smooth shape (4): $\delta \cdot \epsilon \lesssim \tilde{\Delta} \lesssim \delta \Rightarrow \epsilon \lesssim 1$. We thus conclude that a transition between an irregular, sharply folded shape [3] and a smooth superposition (4) occurs at $\epsilon^{SI} \sim O(1)$. A more careful analysis of Euler-Lagrange (EL) equations for the shape (4) reveals that ϵ^{SI} increases with the wavelength contrast ν , and moreover $\epsilon^{SI}(\nu \rightarrow 0) \geq 0.5$ [7]. Since for $\epsilon, \nu \rightarrow \infty$ the shape is characterized by a diverging number of generations of sharp folds [3], we conjecture:

I. *There exists a "branching" series $\{b_n(\epsilon)\}$, such that for (ϵ, ν) with $\epsilon > \epsilon^{SI}(\nu)$, $b_n(\epsilon) < \nu < b_{n+1}(\epsilon)$, the morphological phase is I_n , characterized by n generations of sharp folds.*

Let us focus now on the asymptotic regime ($\nu, \epsilon \ll \epsilon^{SI}(\nu)$), where a smooth shape described by Eq. (4) is expected. We transform now to the dimensionless set:

$$\bar{x} = \frac{x}{l_T}; \quad \bar{y} = \frac{y}{l_T}; \quad \bar{\zeta} = \frac{\zeta}{2l_T \tilde{\Delta}^{1/2}}; \quad \bar{u} = \frac{u}{4\tilde{\Delta} T \epsilon^2}; \quad \bar{\sigma} = \frac{\sigma}{T}; \quad a_j = \sqrt{\epsilon} q_j l_T, \quad (7)$$

where $l_T = \sqrt{T/\rho g}$ and $a_0 = 1$. Eq. (2) yields the EL Eqs.:

$$M(a_0, \bar{x}) \bar{\zeta}_0 - (1 - 2\epsilon a_0^2) \bar{\zeta}_0'' + \epsilon^2 \bar{\zeta}_0'''' = 0 \quad (8)$$

$$M(a_1, \bar{x}) \bar{\zeta}_1 - (1 - 2\epsilon a_1^2) \bar{\zeta}_1'' + \epsilon^2 \bar{\zeta}_1'''' = 0 \quad (9)$$

$$\text{where: } a_0^2 \bar{\zeta}_0(\bar{x})^2 + a_1^2 \bar{\zeta}_1(\bar{x})^2 = 1 \quad (10)$$

$$\text{and: } M(a_i, \bar{x}) \equiv a_i^4 + 1 + \bar{\sigma}(\bar{x}) a_i^2 / \epsilon \quad (11)$$

With the constraint (10), Eqs. (8,9) become a 4th order nonlinear ODE for the function $\bar{\zeta}_0(\bar{x})$ (alternatively, $\bar{\zeta}_1(\bar{x})$), which must be solved under the two BC (6). Obviously, two BC do not suffice to solve a 4th order ODE. One may show, however [7], that in the regime

$$\epsilon \ll 1 \quad ; \quad a_1 \ll 1/\sqrt{\epsilon} \quad , \quad (12)$$

the *minimal energy* profile that satisfy the BC (6) is determined, to leading order in ϵ , by the 2nd order ODE obtained from Eqs. (8,9) after neglecting the 4th derivatives and the terms $2\epsilon a_i^2 \bar{\zeta}_i''$. The BC (6) are thus sufficient for finding the minimal energy profile of the form (4). Physically, this means that force balance in the regime (12) is dominated by tensile forces ($-\bar{\zeta}_i''$) and by the restoring forces associated with variation of the pattern from its preferred wrinkling period ($M(a_i, \bar{x}) \bar{\zeta}_i$), whereas bending forces that result from variation along \hat{x} ($\epsilon^2 \bar{\zeta}_i''''$, $2\epsilon a_i^2 \bar{\zeta}_i''$) are negligible. Let us analyze now the asymptotic behavior of $\bar{\zeta}_0(\bar{x})$, $\bar{\zeta}_1(\bar{x})$. In the limit $\bar{x} \rightarrow \bar{X}_0$ (more generally, for $\bar{x} \ll 1$) we expect $\bar{\sigma}(\bar{x}) \rightarrow -(a_0^2 + a_0^{-2})\epsilon = -2\epsilon$ and from Eq. (11): $M(a_0, \bar{X}_0) = 0$, $M(a_1, \bar{X}_0) = a_1^4 + 1 - 2a_1^2 > 0$.

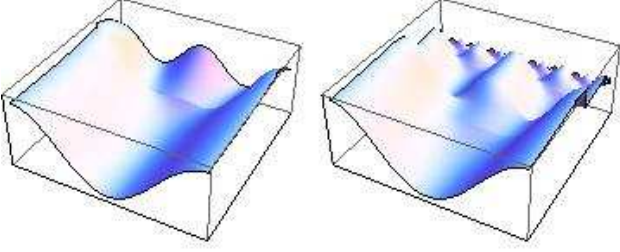


FIG. 2: Computed patterns of wrinkled membranes ($\epsilon \ll 1$), with wavelength contrast $\nu=1$ and a 1-strip shape (left), and with $\nu=15$ and a 4-strip series $q_0(1, 2, 4, 8, 16)$ (right).

In this limit, linear analysis of Eq. (9) implies:

$$\bar{\zeta}_1 = \frac{Q_1}{a_1} \sinh[\sqrt{M(a_1, \bar{X}_0)}(\bar{x} - \bar{X}_0)]; \quad \bar{\zeta}_0 \approx \frac{1 - \frac{1}{2}a_1^2 \bar{\zeta}_1^2}{a_0}, \quad (13)$$

where Q_1 ($\propto e^{-\bar{L}}$) is a constant that is determined by the solution of the nonlinear Eqs. (8-10). The analogous analysis in the limit $\bar{x} \rightarrow \bar{X}_1 = 0$ relies on the assumption $M(a_0, \bar{X}_1) < 0$, that will be justified below. Linear analysis of Eq. (8) near $\bar{x} = \bar{X}_1$ then yields:

$$\bar{\zeta}_0 = \frac{Z_1}{a_0} \sin[\sqrt{M(a_0, \bar{X}_1)}(\bar{x} - \bar{X}_1)]; \quad \bar{\zeta}_1 \approx \frac{1 - \frac{1}{2}a_0^2 \bar{\zeta}_0^2}{a_1}, \quad (14)$$

where Z_1 is another constant. Some algebraic manipulations using Eqs. (6,10,14,8,11) yield:

$$M_-(a_1, a_0, Z_1) \equiv M(a_0, \bar{X}_1) = \frac{a_0^4 + 1 - a_0^2(a_1^2 + \frac{1}{a_1^2})}{1 - Z_1^2(\frac{a_0}{a_1})^2} \quad (15)$$

$$\sigma(\bar{X}_1) = \epsilon[-(a_1^2 + \frac{1}{a_1^2}) + \frac{1}{a_1^2} Z_1^2 M_-(a_1, a_0, Z_1)] \quad (16)$$

With Eq. (15), the asymptotes (13,14), denoted hence as $\bar{\zeta}_i^L(\bar{x})$, $\bar{\zeta}_i^R(\bar{x})$, respectively, are fully described by the two unknown constants Q_1, Z_1 . Although they are the leading terms in asymptotic expansions whose radii of convergence are unknown (and may even vanish), we found an excellent agreement between the function obtained from $\bar{\zeta}_i^L, \bar{\zeta}_i^R$ through standard matching procedure and numerical solution of Eqs. (8-11) (in the regime (12)) for all parameters a_0, a_1 that we tested. Such matching analysis is based on equating $\bar{\zeta}_0^L(\bar{x})$ and $\bar{\zeta}_0^R(\bar{x})$, and their first and second derivatives at an unknown point $\bar{x}^* < \bar{X}_1$. The three matching conditions translate into 3 algebraic equations for the unknowns \bar{x}^*, Z_1, Q_1 , from which expressions for Q_1 and Z_1 as functions of a_0, a_1 , valid in the limit $\epsilon \ll 1$, are derived. Evaluation of the resulting formulas [7] proves that $0 > Z_1(a_0=1, a_1) > -1$ for all $a_1 > 1$, and thus (see Eq. (15)), confirming the assumption $M(a_0, \bar{X}_1) < 0$. A characteristic shape of the form (4) with $a_1=2$ is plotted in Fig. 2. The energetic cost $U(\nu)$ (where $\nu=a_1-1$) of the shape (4) with respect to the 1d periodic wrinkling shape can be calculated (to leading

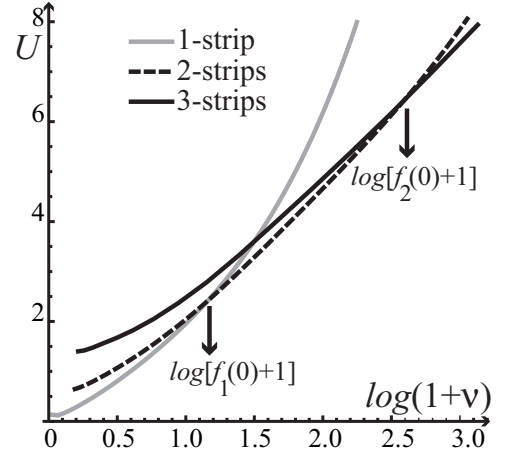


FIG. 3: Energetic costs $U(\nu)$ (for $\epsilon \ll 1$) of symmetric (1-strip), 2-, and 3-strip shapes (obtained by minimizing over all series ($1 > a_1 > a_2 > 1 + \nu$)). Dimensionless convention, Eq. (7), is used.

order in ϵ) by substituting the obtained solutions in Eq. (2). We found the *linear* behavior: $U \approx (\nu - 1)$, plotted as a gray solid line (logarithmic scale) in Fig. 3.

The emergence of intermediate wavenumbers $q_0 < q_i < q_e$ in the wrinkling patterns observed in [4] inspired us to study the stability of the symmetric shape (4) with respect to "n-strip" patterns. A n-strip pattern is defined as n consecutive strips parallel to \hat{y} , with a series of wavenumbers ($q_0 < q_1 \cdots < q_{n-1} < q_n = q_e$), and a series of borderlines (X_1, \cdots, X_{n-1}) (with $X_0 = -L$ and $X_n = 0$), such that the profile in the j^{th} strip is described by a superposition of the type (4) with the change of subscripts:

$$0 \rightarrow j - 1, 1 \rightarrow j. \quad (17)$$

As we now show, the shape in the j^{th} strip, and in particular its length $K_j = \bar{X}_j - \bar{X}_{j-1}$ are determined iteratively from the shape in the $(j-1)^{\text{th}}$ strip by an energetic principle. Let us consider first the vicinity of the borderline $\bar{X}_1 = -K_1$ in a 2-strip shape. We ask whether after the subscripts change (17), the shape can be described by the asymptotics (13) (and $\bar{\zeta}_2(\bar{x})=0$) at $\bar{x} \rightarrow K_1^-$, and by the asymptotics (14) (and $\bar{\zeta}_0(\bar{x})=0$) at $\bar{x} \rightarrow K_1^+$, and a constant Q_2 . Such a shape implies a discontinuity of $\bar{\zeta}_i'(\bar{x})$ at $\bar{x} = K_1$ and hence the divergence of $\bar{\zeta}_i''(\bar{x})$, for $i=0, 2$. These divergences, however, stem from neglecting the 4th derivatives in Eq. (8), and are cured by the formation of a boundary layer of size ϵ around $\bar{x} = K_1$ in which tensile and bending forces ($-\bar{\zeta}_i'', \epsilon^2 \bar{\zeta}_i''''$, respectively) balance each other. Similarly to the "take-off" line that is formed along a paper sheet when it is pushed into a narrow ring, the energetic cost of this layer is negligible for $\epsilon \ll 1$ [7, 8]. Let us consider now $\bar{\zeta}_1(\bar{x})$ near K_1 . Eq. (10) implies $\bar{\zeta}_1'(K_1)=0$ and hence finite values of $\bar{\zeta}_1''(\bar{x})$ at both limits $\bar{x} \rightarrow K_1^+, K_1^-$. If these values are different the 4th derivative $\epsilon^2 \bar{\zeta}_1''''(\bar{x})$ diverges, leading to strong bending force that cannot be balanced by the finite tensile force $\bar{\zeta}_1''(\bar{x})$, and whose existence thus leads to the emergence of a highly energetic region with localized Gaussian curvature, similarly to ridges on crumpled papers [6]. The

“stitching condition”: $\bar{\zeta}_1''(\bar{x} \rightarrow K_1^-) = \bar{\zeta}_1''(\bar{x} \rightarrow K_1^+)$, amounts to the absence of such region. After manipulations similar to those that led to Eq. (15) this condition yields the asymptotics (13) of the second strip at $\bar{x} \rightarrow K_1^+$ with:

$$Q_2 \equiv \sqrt{\frac{-(\frac{a_0}{a_2})^2 M_-(a_1, a_0, Z_1) Z_1^2}{a_2^4 + 1 - a_2^2(a_1^2 + \frac{1}{a_1^2}) + (\frac{a_0}{a_1})^2 M_-(a_1, a_0, Z_1) Z_1^2}} \quad (18)$$

$$M_+(a_2, a_1, Q_2) \equiv M(a_2, \bar{X}_1) = \frac{a_2^4 + 1 - a_2^2(a_1^2 + \frac{1}{a_1^2})}{1 + Q_2^2(\frac{a_2}{a_1})^2} \quad (19)$$

The asymptotics of the second strip at $\bar{x} \rightarrow \bar{X}_2 = 0$ are given by Eqs. (14,17). The unknown constants are now $K_2 = \bar{X}_2 - \bar{X}_1, Z_2$ which can be found by following a matching procedure as described above, or by numerically solving the 2nd order ODE obtained from Eqs. (8 - 10,17) in the regime (12) on an *unknown* interval length K_2 and *three* BC: $\bar{\zeta}_1(\bar{X}_2) = \bar{\zeta}_2(\bar{X}_1) = 0$ and $\bar{\zeta}_2'(\bar{X}_1) = Q_2 \sqrt{M_+(a_2, a_1, Q_2)}$. One thus obtains functional expressions for K_2, Z_2 in terms of a_0, a_1, a_2 . The construction of n -strip with a series ($a_0 = 1 < a_1 < \dots < a_{n-1} < a_n = 1 + \nu$) proceeds iteratively: The shape at the j^{th} strip is fully determined from the known shape in the $(j-1)^{\text{th}}$ strip by an identical procedure to the one described above where the subscript change (17) is supplemented by $2 \rightarrow j+1$. The energy of the n -strip shape is then computed from Eq. (2).

In order to analyze the stability of the symmetric (1-strip) shape with respect to n -strip shapes, we calculated (for $\epsilon \ll 1$) the *minimal* energies of 2- and 3-strip shapes for $\nu \in (0, 20)$. Evaluation of similar plots for $n > 3$ requires elaborate computations, since it involves (for every ν) minimization in a high dimensional ($d \geq 3$) parameter space. We found that both 1-strip and 2-strip energies scale *logarithmically* with ν , such that 1-strip is favorable for $0 < \nu < f_1(0)$, 2-strip is favorable for $f_1(0) < \nu < f_2(0)$, and 3-strip is favorable (over 1- and 2-strip) for $\nu > f_2(0)$, where $f_1(0) \approx 3.2$, $f_2(0) \approx 12$. These observation leads to our second conjecture:

II. *There exists a “period-fissioning” series $\{f_n(\epsilon)\}$, such that for (ϵ, ν) with $\epsilon^{SI}(\nu) < \epsilon < (1+\nu)^2$, $f_n(\epsilon) < \nu < f_{n+1}(\epsilon)$, the phase is F_n , characterized by n -strip shape.*

In Fig. 4 we depict the conjectured irregular ($\{I_n\}$), symmetric (S) and period-fissioning ($\{F_n\}$) phases in the 2d parameter space (ϵ, ν) . As will be shown elsewhere [7], the wrinkling patterns observed in [4] seem to be described by phases F_3 and F_4 . In order to understand

the regime $\epsilon > (1+\nu)^2$, consider Eqs. (16,17). They predict that the compression $|\sigma_{yy}(\bar{x})|$ in the j^{th} strip increases roughly as q_j^2 , and hence imply that the *local* value of ϵ (compression-to-tension ratio) increases and becomes $O(1)$ for $q_j \sim q_0/\sqrt{\epsilon}$. For wavelength contrasts $\nu > \epsilon^{-1/2}$ one may thus expect *mixed phases* ($M_{n,k}$), characterized by n -strip that terminates at $q_j \approx q_0/\sqrt{\epsilon}$, and followed by an irregular shape I_k that terminates at $q_e = (1+\nu)q_0$.

The rich phase space depicted in Fig. 4 describes the morphology of stressed membranes under rather restrictive conditions ($\bar{\Delta} \ll 1$, constant tension, and BC mapped onto a single number ν). Future work will explore

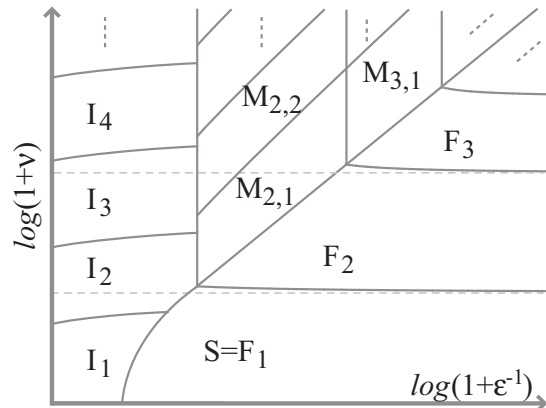


FIG. 4: A conjectured phase diagram for stressed membranes ($\bar{\Delta} \ll 1, \bar{L} \gg 1$). The axis correspond to the dimensionless parameters (ϵ, ν) . The irregular (I_n), period-fissioning (F_n), and mixed ($M_{n,k}$) morphologies are described in the text.

whether morphologies beyond this regime are described by the conjectured phases or whether new phases emerge. Finally, the structure depicted in Fig. 4 raises the speculation that a nontrivial link exists between the irregular ($\{I_n\}$) and period-fissioning ($\{F_n\}$) phases. Computation of the conjectured series $\{b_n(\epsilon), f_n(\epsilon)\}$ may reveal whether this impression is merely a superficial one or points to a deep duality between focusing and uniform distribution of stress in elastic membranes.

Acknowledgments

The author is grateful to D.Nelson and B.Roman for helpful comments, to H.Diamant, I.Dujovne and J.Machta for critical reading of the manuscript, and to N.Menon and C.Santangelo for valuable discussions.

[1] L.D.Landau and L.M.Lifshitz, *Theory of Elasticity* (Pergamon, New York, 1986).
 [2] E.Cerda and L.Mahadevan, Phys. Rev. Lett. **90**, 074302 (2003).
 [3] Y.Pomeau, Phil. Mag. B **78**, 253 (1998); Y.Pomeau and S.Rica, C.R. hebd. Seanc. Acad. Sci. Paris., Ser.IIb **325**, 181 (1997).

[4] J.Huang *et al.*, submitted to Nature Physics.
 [5] L.Pocivavsek *et al.*, Science **320**, 912 (2008).
 [6] T.A.Witten, Rev. Mod. Phys. **79**, 643 (2007).
 [7] In preparation.
 [8] T.Liang and T.A.Witten, Phys. Rev. E **71**, 016612 (2006).